Published by Avanti Publishers

Journal of Advances in Applied & Computational Mathematics

ISSN (online): 2409-5761

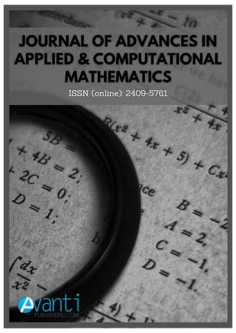

Rocking Response of the Rigid Block Under Rectangular Pulse Excitation: A Comparison between ODE and Optimization-Based Solvers

R. Gagliardo, F.P.A. Portioli*, L. Cascini and R. Landolfo

Department of Structures for Engineering and Architecture, University of Naples Federico II, via Forno Vecchio 36, 80134, Naples, Italy

ARTICLE INFO

Article Type: Research Article

Keywords:
Rocking
Rigid block
ODE solver
Mathematical programming
Differential equation of motion

Timeline:
Received: June 06, 2021
Accepted: August 11, 2021
Published: December 31, 2021

Citation: Gagliardo R, Portioli FPA, Cascini L, Landolfo R. Rocking Response of the Rigid Block Under Rectangular Pulse Excitation: A Comparison between ODE and Optimization-Based Solvers. J Adv App Comput Math. 2021; 8: 109-116.

DOI: https://doi.org/10.15377/2409-5761.2021.08.8

ABSTRACT

In this paper, the response of the rigid block under rectangular pulse excitation is investigated using two different modeling approaches and solvers. The first approach relies on the numerical integration of the differential equation of motion. The second approach is based on the formulation of the dynamic problem in terms of a special class of mathematical programming problem that is the linear complementarity problem. A validation study is carried out comparing the solutions given by the proposed formulation with the ones given by the numerical integration of the differential equation of motion obtained from ODE solvers available in MATLAB®. Potentialities and limitations of the mathematical programming formulation are discussed in terms of energy dissipation and restitution coefficient at impacts and in terms of solution times.

*Corresponding Author
Email: fportiol@unina.it
Tel: +39 081 2538916

1. Introduction

The assessment and evaluation of rocking response of rigid blocks under ground excitation is a topic investigated mainly within the framework of structural researchers, considering that it is a suitable modeling approach to analyze the seismic structural capacity of a large variety of structures. Historic masonry structures, which usually do not exhibit a box behavior, can be conveniently modeled as an assemblage of rigid parts, the so-called macro-elements. As a matter of fact, the rocking failure modes of macro-elements effectively assess the structural capacity of ancient masonry buildings under seismic actions [1]. The rocking response of rigid blocks can be handled numerically, starting from the position of the equation of motions. In the case of a single rigid block, the typical motion of the rocking block is an alternate rotation of the block around two vertexes at the base. At each ground impact, the block dissipates a certain amount of energy, the angular velocity decreases, and the rotation reverses. The amount of energy loss per impact is a function of the block slenderness and of the properties of the contact at the base. Plastic deformations may occur at contact points, but the corresponding amount of energy loss is usually neglected in the formulations [2,3].

Several approaches and formulations have been proposed in the scientific literature. Among others, it is worth mentioning the seminal work by Housner [4], who first proposed to analyze the dynamic behavior of the rocking blocks by posing the formulation of the inverted pendulum. The author defined the equation of motion of a rocking block under the assumption of a fully rigid model where displacements arise soon after the activation of rocking motion. Starting from this study, many other formulations have been developed with the aim to step forward Housner's assumptions and move towards the analysis of multiple-blocks structure, also considering flexible foundations or deformable blocks. Further details can be found in [4-7].

In recent times, force-based and displacement-based approaches, either in the static or dynamic field, have been developed to assess the rocking response t of historic masonry structures[8-16]. Many literature applications in the field of seismic assessment are based on the development of the finite element method (FEM) and distinct element method (DEM) [17,18]. Nevertheless, an emerging and valid alternative is the Non-Smooth Contact Dynamics (NSCD) method, which poses the problem of the dynamic of rocking motions in terms of mathematical programming problem: equilibrium equations and complementary conditions are given at contact points, and the dynamic solution is found by using optimization methods for which, nowadays, efficient solvers exist [19-24]. The possibility to adopt mathematical programming methods for the equilibrium analysis of rigid blocks was firstly investigated in [25] within the field of limit analysis. Since then, many approaches have been developed [26-32], formulating the different types of contact model, flow rule, and involved failure conditions. A fundamental contribution was provided in [33,34], where the overall system for the solution of the problem was presented in terms of a linear complementary problem. Significant advancements were presented [35,36] where the Authors showed the possibility to express the linear complementary problem in terms of dual quadratic programming problems, corresponding to a force-based and a displacement-based problem, respectively.

Within this framework, this paper presents an application of the formulation proposed in [32,37] to analyze the rocking response of a wall subjected to rectangular pulse excitations using mathematical programming. The novel contribution of the present study is related to the evaluation of the numerical damping, which is implicitly associated in the considered configuration, to the adopted time-stepping scheme for the integration of the equations of motion. The wall is modeled as a single rigid block, and a support block is used to apply the acceleration time history. The results obtained from the numerical formulation based on mathematical programming are compared with those obtained from the numerical integration of the differential equation of motion. The comparison is carried out in terms of rotation and angular velocity time history. A sensitivity analysis was carried out on the numerical model based on mathematical programming to investigate the influence of the time step size on the energy dissipation associated with the adopted time-stepping scheme.

The paper is organized as follows. In Section 2, the ordinary differential equation (ODE) in the case of the rocking motion of a rigid rectangular block is described. The proposed numerical formulation of the mathematical programming problem for the dynamic analysis is presented in Section 3, as well as the incremental solution procedure adopted for the analysis of the dynamic contact response among the two following steps. Finally, the

outcomes obtained by using ODE and the proposed optimization problem are compared in Section 4 concerning the case study of a free-standing wall subjected to rectangular pulse excitation.

2. The Differential Equation of Motion of the Rigid Block

It is well known from the literature that, for rectangular blocks, the equation of the rocking motion about the center of rotations at the base can be posed in compact form as follows, assuming that no sliding occurs [38]:

$$\ddot{\omega}(t) = -p^2 \left\{ sin[\varphi \mathrm{sgn}[\omega(t)] - \omega(t)] + \frac{a_g}{g} cos[\varphi \mathrm{sgn}[\omega(t)] - \omega(t)] \right\} \quad (1)$$

where ω is the rotation angle, $\varphi = tan^{-1}(b/h)$ is the slenderness angle, $p = \sqrt{\frac{3g}{4R}}$ is the frequency parameter, and R is the radial distance of the block (Fig. **1**).

Considering conservation of momentum before and after the impacts, the ratio of kinetic energy measuring the minimum energy loss with rigid contacts can be expressed as:

$$r = \left(1 - \frac{3}{2} sin^2(\varphi)\right)^2, \quad (2)$$

r being the coefficient of restitution of kinetic energy.

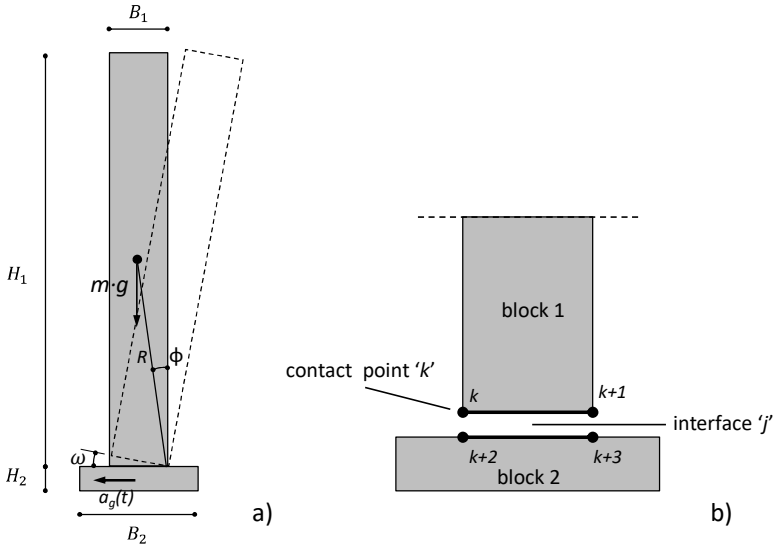

Figure 1: a) Rigid block model of the free rocking wall with support block; b) location of contact points at interface '*j*'.

The *ode45* solver available in MATLAB® was used for numerical integration of (1). The solver is based on a Runge-Kutta integration scheme. To take into account the impacts and corresponding energy dissipation during rocking motion, an event-driven algorithm was implemented. After the time of impact corresponding to a rotation angle equal to zero, the equation of motion is integrated on the basis of the angular velocity right after the impact. This velocity is obtained as follows:

$$\frac{\dot{\omega}_2}{\dot{\omega}_1} = \sqrt{r}, \quad (3)$$

being $\dot{\omega}_2$ and $\dot{\omega}_1$ the angular velocity just after and before the impact.

3. Formulation of the Rocking Response in Terms of Optimization Problems

In this section, the discretized variational formulation of the equation of motion is presented. The formulation relies on a discrete numerical model, which includes two rigid blocks representing the rocking wall and the

support block (block 1 and block 2 in Fig. **1a**). Pulse excitations are applied at support block 2. The rigid blocks interact at two contact interfaces *j*: the first one between block 1 and block 2 is a frictional contact interface while the second one, between block 2 and the ground, is a frictionless interface. Each contact interface comprises four contact points *k*,...*k*+3, as shown in Fig. **1b**. For each contact point, a normal force, orthogonal to the contact surface, and a shear force are defined. Assuming an infinite compressive strength and a no-tension behavior, the present formulation includes three possible failure conditions at each contact point: opening, positive and negative sliding, which follow the Coulomb friction law. The relationship between internal forces and corresponding contact displacement rates at failure follows the rule of associative behavior in sliding: once internal forces at a contact point attain ultimate capacity, the corresponding sliding displacement leads to dilatancy. Such an assumption dramatically simplifies the mathematical position of the problem so that the kinematic behavior of contact points at failure can be expressed in terms of a flow rule matrix, which is simply the transpose of the matrix governing failure conditions, times the vector of flow multipliers. Considering that, in case of normal displacements, contact opening only is admitted, while the possibility of penetration at contact is prevented, a vector of initial gaps is introduced in the formulation to ensure that normal forces at contact occur only if the gap between two contact points is closed.

As such, the matrix form of the equation system governing the rocking response of the wall can be posed in terms of a linear complementarity problem (LCP), as follows [32]:

$$\begin{bmatrix} \bar{\boldsymbol{M}} & . & \boldsymbol{A_0} \\ . & . & -\boldsymbol{Y}^{\mathrm{T}} \\ -\boldsymbol{A_0}^{\mathrm{T}} & \boldsymbol{Y} & . \end{bmatrix}_{n\times n} \begin{bmatrix} \boldsymbol{\Delta x} \\ \boldsymbol{\lambda} \\ \boldsymbol{c} \end{bmatrix}_{n\times 1} + \begin{bmatrix} . \\ \boldsymbol{y} \\ . \end{bmatrix} = \begin{bmatrix} \bar{\boldsymbol{f}}_{\boldsymbol{0}} \\ . \\ -\boldsymbol{g_0} \end{bmatrix}, \quad \text{s.t.} \quad \boldsymbol{y} \le \boldsymbol{0} \quad \boldsymbol{\lambda} \ge \boldsymbol{0} \quad \boldsymbol{y}^{\mathrm{T}}\boldsymbol{\lambda} = 0 \tag{4}$$

where:

$\boldsymbol{\Delta x}$: is the vector of displacement rates at block centroids;

$\boldsymbol{c}$: is the vector of contact forces;

$\boldsymbol{g_0}$: is the vector of contact gaps;

$\bar{\boldsymbol{f}}_{\boldsymbol{0}}$: is the vector of external scaled forces;

$\boldsymbol{y}$: is the vector of failure conditions;

$\boldsymbol{\lambda}$: is the vector of non-negative flow multipliers;

$\boldsymbol{A_0}$: is the equilibrium matrix;

$\bar{\boldsymbol{M}}$: is the scaled mass matrix;

$\boldsymbol{Y}$: is the flow rule matrix.

The rows of the matrix $M \in R^{n\times n}$ associated to the LCP correspond to, respectively: equilibrium conditions; failure conditions; the flow rule, expressing the relative displacement rates at contact interfaces as a function of the displacement rates at block centroids and the vector of flow multipliers.

A time-stepping scheme was used for the integration of the equation of motion, which is based on the implicit Euler method, assuming that at time $t = t_0 + \Delta t$ accelerations and velocities are expressed as $\boldsymbol{a}(t) = \frac{\boldsymbol{v}-\boldsymbol{v_0}}{\Delta t}$ and $\boldsymbol{v}(t) = \frac{\boldsymbol{\Delta x}}{\Delta t}$, respectively, being $\boldsymbol{v_0}$ the initial velocity at time t_0. The vector $\boldsymbol{\Delta x} = \boldsymbol{x} - \boldsymbol{x_0}$ collects the displacement rates of the two blocks centroids that is simply the difference between the position $\boldsymbol{x}$ of each centroid at the time t and their initial position $\boldsymbol{x_0}$ at the beginning of the analysis.

Based on the adopted integration method, the scaled mass matrix and the scaled vector of external forces can be expressed on the basis of the corresponding matrix $\boldsymbol{M}$ and vector $\boldsymbol{f}$ as follows: $\bar{\boldsymbol{M}} = \frac{1}{\Delta t^2}\boldsymbol{M}$ and $\bar{\boldsymbol{f}}_{\boldsymbol{0}} = \boldsymbol{f} + \bar{\boldsymbol{M}}\boldsymbol{v_0}\Delta t$.

Problem (4) is equivalent to the two dual quadratic optimization problems:

$$\begin{aligned} \min \quad & \tfrac{1}{2}\boldsymbol{\Delta x}^{\mathrm{T}}\,\bar{\boldsymbol{M}}\boldsymbol{\Delta x} - \bar{\boldsymbol{f}}_{\boldsymbol{0}}^{\mathrm{T}}\boldsymbol{\Delta x} \\ \text{s.t.} \quad & \boldsymbol{\Delta u} = \boldsymbol{A}_{\boldsymbol{0}}^{\mathrm{T}}\,\boldsymbol{\Delta x} \\ & \boldsymbol{\Delta u} = \boldsymbol{Y\lambda} + \boldsymbol{g}_{\boldsymbol{0}}, \boldsymbol{\lambda} \geq \boldsymbol{0} \end{aligned} \quad , \tag{5}$$

and

$$\begin{aligned} \max \quad & -\tfrac{1}{2}\boldsymbol{i}^{\mathrm{T}}\,\bar{\boldsymbol{M}}^{-\boldsymbol{1}}\boldsymbol{i} - \boldsymbol{g}_{\boldsymbol{0}}^{\mathrm{T}}\boldsymbol{c} \\ \text{s.t.} \quad & \boldsymbol{i} + \boldsymbol{A}_{\boldsymbol{0}}\boldsymbol{c} = \bar{\boldsymbol{f}}_{\boldsymbol{0}} \\ & \boldsymbol{y} \leq \boldsymbol{0}, \boldsymbol{y} = \boldsymbol{Y}^{\mathrm{T}}\boldsymbol{c} \end{aligned} \quad , \tag{6}$$

where $\boldsymbol{i} = \bar{\boldsymbol{M}}\boldsymbol{\Delta x}$ is the vector of the scaled inertia forces.

The scheme is based on the solution of the force-based problem (6) at the time step t_0, with unknown inertia forces $\boldsymbol{i}$ and contact forces $\boldsymbol{c}$ and known configuration $\boldsymbol{x_0}$, velocities $\boldsymbol{v_0}$ and scaled forces $\bar{\boldsymbol{f}}_{\boldsymbol{0}}$. The displacement rates at block centroid $\boldsymbol{\Delta x}$ are derived from the solution of problem (5), which is directly obtained from Lagrange multipliers associated with the solution of the problem (6). The new position of the blocks and velocities, contact gaps, and external forces are determined, and a new optimization problem (6) is formulated at time increment $t_0 + \Delta t$ on the basis of updated configuration.

4. Numerical Comparisons

The response obtained from the solution of the ODE (1) and the optimization problems (5), (6) was compared for the free-standing wall shown in Fig. **1** subjected to rectangular pulse excitation. The wall dimensions were $B_1 = 0.50\ m$ and $H_1 = 3.50\ m$. In the numerical model, a friction coefficient equal to 0.6 was assumed to prevent sliding between the rocking wall and the support block.

Fig. **2a** shows the comparison of the responses for a rectangular pulse with a magnitude $a_g = 0.20g$ and duration 0.15 sec. The ODE of motion was integrated assuming for the angular coefficient of restitution $\sqrt{r} = 0.95$. The comparison in terms of angular velocity time history is also shown in Fig.**3a**, where the discontinuities at impacts correspond to the kinetic energy loss.

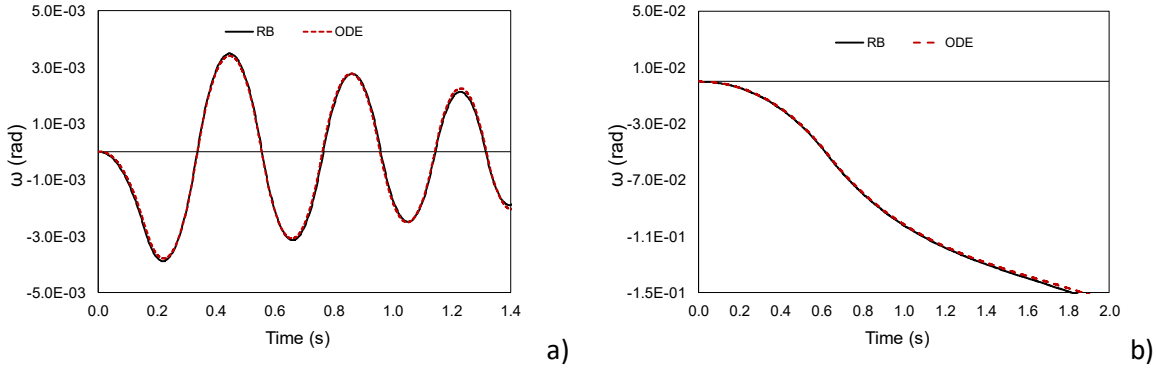

Figure 2: Comparison of rotation time histories for a rectangular pulse with magnitude a_g=0.20g and: a) duration equal to 0.15s; b) duration equal to 0.62s.

A comparison of the pulse duration involving the overturning of the wall was also carried out. In Fig. **2b**, the responses obtained for a pulse with the same magnitude and duration equal to 0.62 sec. are reported.

In the adopted non-smooth contact dynamic formulation, the dissipation depends upon the algorithm and is implicitly related to the time-stepping scheme used for integration. In Fig. **3b**, the sensitivity of the angular

coefficient of restitution to the size of time increment is shown. It can be noted that the angular coefficient of restitution $\sqrt{r}$ (corresponding to the line indicated with 'Analytical' in Fig. **3b**) represents an upper bound to the numerical coefficient of restitutions corresponding to different time-step sizes. A comparison in terms of CPU time was also carried out using a PC equipped with a 3.3 GHz Intel Xeon E3-1245 processor with 8 GB of RAM. The results show that CPU time for the optimization-based formulation is up to two orders of magnitude longer than that required by the ODE solver for a time step of 0.001 sec and decreases by one order of magnitude for a step size of 0.008 sec.

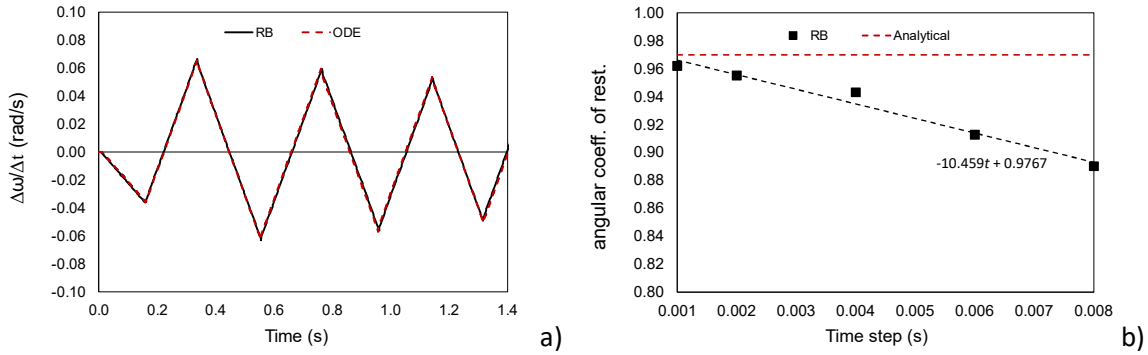

Figure 3: a) Comparison of angular velocities time histories for impulse duration equal to 0.15s; b) Sensitivity analysis of the angular coefficient restitution with a varying time step size.

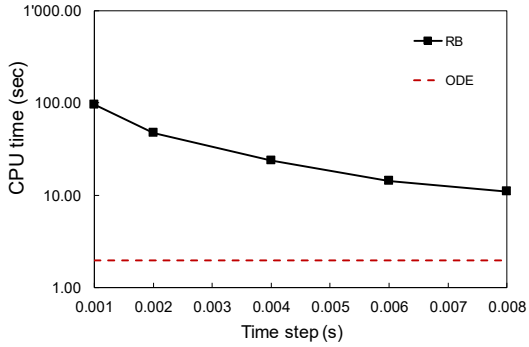

Figure 4: Comparison of CPU times of proposed RB model with MATLAB® ODE solver.

5. Conclusions

The rocking responses of a free-standing wall subjected to rectangular pulse excitation were investigated using the differential equation of motion and a dynamic contact formulation expressed in terms of optimization problems. Different durations of the acceleration pulse were considered to compare the responses in the case of free rocking motion and incipient overturning.

The comparison showed that the numerical response obtained from the mathematical programming formulation is in good agreement with that obtained from the numerical integration of the differential equation of motion.

Although the adopted variational formulation takes into account non-smooth events associated with impacts in a compact, general form, the energy dissipation remains implicitly related to the algorithm used for time integration and, in particular, to the size of the time increment.

The comparison between the differential equation of motion and the adopted dynamic formulation was finally performed in terms of computational efficiency. Solution times for the variational formulation were found to be

up to two orders of magnitude longer than those needed by the ODE solver for the shortest time step size considered. Increasing the time step size in the numerical integration scheme used for the optimization problem also reduces computational costs of about one order of magnitude.

Acknowledgments

The financial support of the research project DPC-ReLUIS: Work Package 5 'Integrated and low-impact strengthening interventions' (2019-2021) is acknowledged.

References

[1] Lagomarsino S. Seismic assessment of rocking masonry structures. Bull Earthq Eng 2015;13:97-128. https://doi.org/10.1007/s10518-014-9609-x.

[2] Makris N, Roussos Y. Rocking Response and Overturning of Equipment Under Horizontal Pulse-Type Motions. Pacific Earthquakes, Eng Res Cent 1998. https://doi.org/10.13140/rg.2.1.1207.0566.

[3] Makris N, Zhang J. Rocking Response and Overturning of Anchored Equipment under Seismic Excitations. Pacific Earthq Eng Res Cent 1999:1-82.

[4] Spanos PD, Koh A-S. Rocking of rigid blocks due to harmonic shaking. J Eng Mech 1984;110:1627-42. https://doi.org/10.1061/(ASCE)0733-9399(1984)110:11(1627).

[5] Psycharis IN, Jennings PC. Rocking of slender rigid bodies allowed to uplift. Earthq Eng & Struct Dyn 1983;11:57-76. https://doi.org/10.1002/eqe.4290110106.

[6] Ishiyama Y. Motions of rigid bodies and criteria for overturning by earthquake excitations. Earthq Eng & Struct Dyn 1982;10:635-50. https://doi.org/10.1002/eqe.4290100502.

[7] Aslam M, Fodden WG, Scalise DT. Earthquake rocking response of rigid bodies. J Struct Div ASCE 1980;106:377-92.

[8] Malomo D, Mehrotra A, DeJong MJ. Distinct element modeling of the dynamic response of a rocking podium tested on a shake table. Earthq Eng Struct Dyn 2021;50:1469-75. https://doi.org/10.1002/eqe.3404.

[9] Grillanda N, Chiozzi A, Milani G, Tralli A. Tilting plane tests for the ultimate shear capacity evaluation of perforated dry joint masonry panels. Part II: Numerical analyses. Eng Struct 2021;228. https://doi.org/10.1016/j.engstruct.2020.111460.

[10] Giresini L, Solarino F, Paganelli O, Oliveira DV, Froli M. ONE-SIDED rocking analysis of corner mechanisms in masonry structures: Influence of geometry, energy dissipation, boundary conditions. Soil Dyn Earthq Eng 2019;123:357-70. https://doi.org/10.1016/j.soildyn.2019.05.012.

[11] Giouvanidis AI, Dong Y. Seismic loss and resilience assessment of single-column rocking bridges. Bull Earthq Eng 2020;18:4481-513. https://doi.org/10.1007/s10518-020-00865-5.

[12] Giouvanidis AI, Dimitrakopoulos EG. Rocking amplification and strong-motion duration. Earthq Eng Struct Dyn 2018;47:2094-116. https://doi.org/10.1002/eqe.3058.

[13] Galassi S, Ruggieri N, Tempesta G. A Novel Numerical Tool for Seismic Vulnerability Analysis of Ruins in Archaeological Sites. Int J Archit Herit 2020;14:1-22. https://doi.org/10.1080/15583058.2018.1492647.

[14] Funari MF, Mehrotra A, Lourenço PB. A tool for the rapid seismic assessment of historic masonry structures based on limit analysis optimisation and rocking dynamics. Appl Sci 2021;11:1-22. https://doi.org/10.3390/app11030942.

[15] De-Felice G, Malena M. Failure pattern prediction in masonry. J Mech Mater Struct 2019;14:663-82. https://doi.org/10.2140/jomms.2019.14.663.

[16] Casapulla C, Giresini L, Lourenço PB. Rocking and kinematic approaches for rigid block analysis of masonry walls: State of the art and recent developments. Buildings 2017;7. https://doi.org/10.3390/buildings7030069.

[17] Acary V, Brogliato B. Numerical methods for non-smooth dynamical systems. Berlin: Springer; 2008.

[18] Jean M. The non-smooth contact dynamics method. Comput Methods Appl Mech Eng 1999;177:235-57. https://doi.org/10.1016/S0045-7825(98)00383-1.

[19] Rafiee A, Vinches M, Bohatier C. Modelling and analysis of the Nîmes arena and the Arles aqueduct subjected to a seismic loading, using the Non-Smooth Contact Dynamics method. Eng Struct 2008;30:3457-67. https://doi.org/10.1016/j.engstruct.2008.05.018.

[20] Lancioni G, Lenci S, Piattoni Q, Quagliarini E. Dynamics and failure mechanisms of ancient masonry churches subjected to seismic actions by using the NSCD method: The case of the medieval church of S. Maria in Portuno. Eng Struct 2013;56:1527-46. https://doi.org/10.1016/j.engstruct.2013.07.027.

[21] Andersen ED, Roos C, Terlaky T. On implementing a primal-dual interior-point method for conic quadratic optimization. Math Program Ser B 2003;95:249-77. https://doi.org/10.1007/s10107-002-0349-3.

[22] Tasora A, Anitescu M. A matrix-free cone complementarity approach for solving large-scale, nonsmooth, rigid body dynamics. Comput Methods Appl Mech Eng 2011;200:439-53. https://doi.org/10.1016/j.cma.2010.06.030.

[23] Stewart DE, Trinkle JC. An implicit time-stepping scheme for rigid body dynamics with inelastic collisions and coulomb friction. Int J Numer Methods Eng 1996;39:2673-91. https://doi.org/10.1002/(SICI)1097-0207(19960815)39:15<2673::AID-NME972>3.0.CO;2-I.

[24] Anitescu M, Potra FA. A time-stepping method for stiff multibody dynamics with contact and friction. Int J Numer Methods Eng 2002;55:753-84. https://doi.org/10.1002/nme.512.

[25] Livesley RK. Limit analysis of structures formed from rigid blocks. Int J Numer Methods Eng 1978;12:1853-71. https://doi.org/10.1002/nme.1620121207.

[26] Baggio C, Trovalusci P. Limit analysis for no-tension and frictional three-dimensional discrete systems. Mech Struct Mach 1998;26:287-304. https://doi.org/10.1080/08905459708945496.

[27] Baggio C, Trovalusci P. Collapse behavior of three-dimensional brick-block systems using non-linear programming. Struct Eng Mech 2000;10:181-95. https://doi.org/10.12989/sem.2000.10.2.181.

[28] Cascini L, Gagliardo R, Portioli F. LiABlock_3D: A Software Tool for Collapse Mechanism Analysis of Historic Masonry Structures. Int J Archit Herit 2020;14:75-94. https://doi.org/10.1080/15583058.2018.1509155.

[29] Orduña A, Lourenço PB. Three-dimensional limit analysis of rigid blocks assemblages. Part I: Torsion failure on frictional interfaces and limit analysis formulation. Int J Solids Struct 2005;42:5140-60. https://doi.org/10.1016/j.ijsolstr.2005.02.010.

[30] Orduña A, Lourenço PB. Three-dimensional limit analysis of rigid blocks assemblages. Part II: Load-path following solution procedure and validation. Int J Solids Struct 2005;42:5161-80. https://doi.org/10.1016/j.ijsolstr.2005.02.011.

[31] Portioli F, Casapulla C, Cascini L. An efficient solution procedure for crushing failure in 3D limit analysis of masonry block structures with non-associative frictional joints. Int J Solids Struct 2015;69-70:252-66. https://doi.org/10.1016/j.ijsolstr.2015.05.025.

[32] Portioli FPA. Rigid block modeling of historic masonry structures using mathematical programming: a unified formulation for non-linear time history, static pushover, and limit equilibrium analysis. Bull Earthq Eng 2020;18:211-39. https://doi.org/10.1007/s10518-019-00722-0.

[33] Fishwick RJ. Limit analysis of rigid block structures—University of Portsmouth, 1996.

[34] Ferris MC, Tin-Loi F. Limit analysis of frictional block assemblies as a mathematical program with complementarity constraints. Int J Mech Sci 2001;43:209-24. https://doi.org/10.1016/S0020-7403(99)00111-3.

[35] Krabbenhoft K, Huang J, Da Silva MV, Lyamin AV. Granular contact dynamics with particle elasticity. Granul Matter 2012;14:607-19. https://doi.org/10.1007/s10035-012-0360-1.

[36] Lim K-W, Krabbenhoft K, Andrade JE. A contact dynamics approach to the Granular Element Method. Comput Methods Appl Mech Eng 2014;268:557-73. https://doi.org/10.1016/j.cma.2013.10.004.

[37] Portioli F, Cascini L. Contact Dynamics of Masonry Block Structures Using Mathematical Programming. J Earthq Eng 2018;22:94-125. https://doi.org/10.1080/13632469.2016.1217801.

[38] Zhang J, Makris N. Rocking response of free-standing blocks under cycloidal pulses. J Eng Mech 2001;127:473-83. https://doi.org/10.1061/(ASCE)0733-9399(2001)127:5(473).